

A differential photodetector: Detecting light modulations using transient photocurrents

Cite as: AIP Advances 6, 015306 (2016); <https://doi.org/10.1063/1.4939921>

Submitted: 17 November 2015 . Accepted: 30 December 2015 . Published Online: 11 January 2016

Louisa Reissig, Simon Dalgleish, and Kunio Awaga



View Online



Export Citation



CrossMark

ARTICLES YOU MAY BE INTERESTED IN

[Optoelectronic conversion by polarization current, triggered by space charges at organic-based interfaces](#)

Applied Physics Letters **96**, 243303 (2010); <https://doi.org/10.1063/1.3454915>

[Electric double layers allow for opaque electrodes in high performance organic optoelectronic devices](#)

Applied Physics Letters **101**, 173302 (2012); <https://doi.org/10.1063/1.4762823>

[Highly efficient organic optoelectronic conversion induced by electric double layers in ionic liquids](#)

Applied Physics Letters **100**, 163304 (2012); <https://doi.org/10.1063/1.3697988>

NEW

AVS Quantum Science

A new interdisciplinary home for impactful quantum science research and reviews

Co-Published by

NOW ONLINE

A differential photodetector: Detecting light modulations using transient photocurrents

Louisa Reissig,^{1,a} Simon Dalglish,^{1,2} and Kunio Awaga^{1,3,b}

¹*Department of Chemistry and Research Centre for Material Science, Nagoya University, Furo-cho, Chikusa-ku, 464-8602 Nagoya, Japan*

²*Institute for Advanced Research, Nagoya University, Furo-cho, Chikusa-ku, 464-8601 Nagoya, Japan*

³*CREST, JST, Nagoya University, Furo-cho, Chikusa-ku, 464-8602 Nagoya, Japan*

(Received 17 November 2015; accepted 30 December 2015; published online 11 January 2016)

Inserting an insulating layer (I) into a conventional metal-semiconductor-metal (MSM) photodiode converts the DC photoresponse into a strong transient signal, highly applicable to modulated signal photodetection. In this study, we demonstrate the intrinsic benefits of organic MISM photodetectors, namely their effective operation under high steady-state lighting, responding only to changes in light intensity, and their ability to react to several light sources simultaneously. Furthermore, the strong interaction at the S/I interface, specific to this architecture, significantly enhances the device photoresponse, resulting in highly efficient differential photodetection, compared to a composite MSM + C device fabricated from identical elements. © 2016 Author(s). All article content, except where otherwise noted, is licensed under a Creative Commons Attribution (CC BY) license (<http://creativecommons.org/licenses/by/4.0/>). [<http://dx.doi.org/10.1063/1.4939921>]

In our everyday life, we are surrounded by increasing numbers of electronic devices, including displays, sensors, transducers, etc. While most of these devices are based on inorganic semiconductors, such as silicon or germanium, organic materials have received increasing attention due to their low cost, light weight, flexibility, and ease of fabrication, and, despite their comparably low performance, several commercial products based on organic materials are now emerging.¹ Especially for optoelectronic applications, in which light is converted to/from electrical energy, organic materials are attractive due to the indefinite ability of tuning their band gap ($\Delta\text{HOMO} - \text{LUMO}$) to absorb or emit light at almost any wavelength, by tuning their chemical structure and/or intermolecular interactions.^{2,3} However, in order to reap the benefits of organic materials to the fullest, device architectures that exploit their advantages, rather than tolerate their shortcomings as inorganic analogues, are necessary in order to yield competitive devices, as well as to develop novel functions.

In recent years, much attention has focused on the photocurrent response of one or more organic semiconducting layers (S) sandwiched between two metal electrodes (M), which generates a constant DC response upon constant illumination (as in a solar cell) or an ON-OFF DC signal to light pulses (as in photodetectors).⁴⁻⁷ In both cases, the number and nature of the charge transporting layers has been progressively tuned to ensure uni-directionality of the response and/or increased signal strength. In 2010, a novel photodetector architecture was proposed in which a thick insulating layer (I) was introduced between the photoactive semiconducting layer and one of the metal electrodes.⁸ While this additional layer in the so-called MISM device essentially blocks the DC current component, and is, therefore, not immediately applicable to solar cells, the resulting signal is in the form of an intense transient photocurrent peak of opposite polarity for light ON and OFF signals. To date, such photodetectors, with bandwidths up to 1 MHz

^aAuthor to whom correspondence should be addressed. Electronic mail: Louisa_Reissig@gmx.de

^bAuthor to whom correspondence should be addressed. Electronic mail: awaga@mbox.chem.nagoya-u.ac.jp

operating at communication relevant wavelengths, could be fabricated, even for low mobility semiconductors,⁹ and with more optimized device and semiconductor design, higher speeds can be anticipated. Furthermore, the use of ionic liquids (IL) as the insulating layer has significantly increased the responsivity of these IL-MISM devices to 272 mA/W,¹⁰ without applied bias, comparable to commercially available silicon photodiodes, with high stability and high reproducibility.¹¹

In this study, we demonstrate the secondary functions specific to MISM photodetectors, such as the operation under strong background illumination, and the simultaneous detection of several modulated light sources. These experiments not only open up new avenues of application for the MISM photodetectors, but clarify their mechanism of operation. An equivalent circuit is proposed that has helped with the interpretation of signal shape, and has led to new strategies for the development of faster photodetectors of higher responsivity. Furthermore, the results show that the strong interplay between the adjacent layers can enhance the performance, compared to a circuit made from discrete components.

For the purposes of this study, planar MISM devices utilizing an ionic liquid as the insulating layer (IL-MISM)¹¹ were taken, in conjunction with the well-studied heterojunction blend system of poly(3-hexylthiophene):[6,6]-phenyl-C₆₁-butyric acid methyl ester (P3HT:PCBM, 1:1) as the photoactive semiconductor layer (Figure 1(a) and Supporting Information¹⁸ Figure S1).¹⁰ Such a planar architecture has proved remarkably stable,¹¹ and the relatively slow waveform, deliberately induced by the large electrode offset, means that architectural effects on the resultant waveform can be readily identified, free from effects of the external circuitry or measurement apparatus. The results described here could be reproduced with a number of devices initially fabricated for a parallel study focusing on the stability of the devices, the effect of electrode materials, the active layer composition (including blend/bilayer arrangements), and the nature of the ionic liquids used. The ionic liquids, electrode materials and blend composition stated below are only for the devices specifically shown in the manuscript, but the functionality of the devices are independent of the specific design. All devices tested were stable over several weeks/month, yielding responsivities up to 115 mA/W at 530 nm at a light power of 1 mW/cm² (reduced from maximum¹⁰ due to the large electrode offset¹¹), with minimal degradation over this period.

When light falls onto a commercial silicon photodiode (representative for an MSM device), a steady-state current signal is generated, proportional to the intensity of light (Supporting Information¹⁸ Figure S2), and thus the increase or decrease of the light intensity leads simply to a change in magnitude of the photocurrent signal (Figure 1(b)). In contrast, the MISM photodetector responds to switching the light ON or OFF by displaying positive or negative transients, respectively (Figure 1(c)). A further positive transient can be observed if the light intensity is abruptly further increased, while negative transients occur upon stepwise decreases in light intensity. In other words the MISM photodetector responds to fast and stepwise changes in light intensity, and is (after its initial transient) insensitive to constant light. Although the dependence of signal height, and especially moved charge, has an increasingly sub-linear dependence on light intensity, and the height/shape of the second transient is influenced by the first (*vide infra*), the sharp nature of the signal can still be easily resolved.

This quasi-insensitivity to background light allows the operation of the MISM photodetector under daylight/room lightening and, furthermore, it can be used to simultaneously detect signals of two superimposed light sources operating at the same wavelength but at different frequencies (Figure 1(d)). This opens the possibility of changing the encryption of information from the frequency domain to amplitude modulation defining binary code, as a 111 000 sequence can be easily transmitted through 3 increases in light intensity, followed by 3 decreases (Figure 1(c)). Furthermore, to transmit different light sources of different frequencies, no change in wavelength is required, as is commonly done in multiplexing.¹²

In addition, the high sensitivity of the MISM photodetector to small fluctuations in light intensity is corroborated by looking at the “invisible” flickering of a commercial filament bulb (Figure 1(e)). The spike-like shape of the signal, and the removal of the baseline-shift, facilitates the triggering on the fluctuations, when compared to the silicon photodiode (Supporting Information¹⁸ Figure S3). While the study and characterization of such flickering might provide a general platform

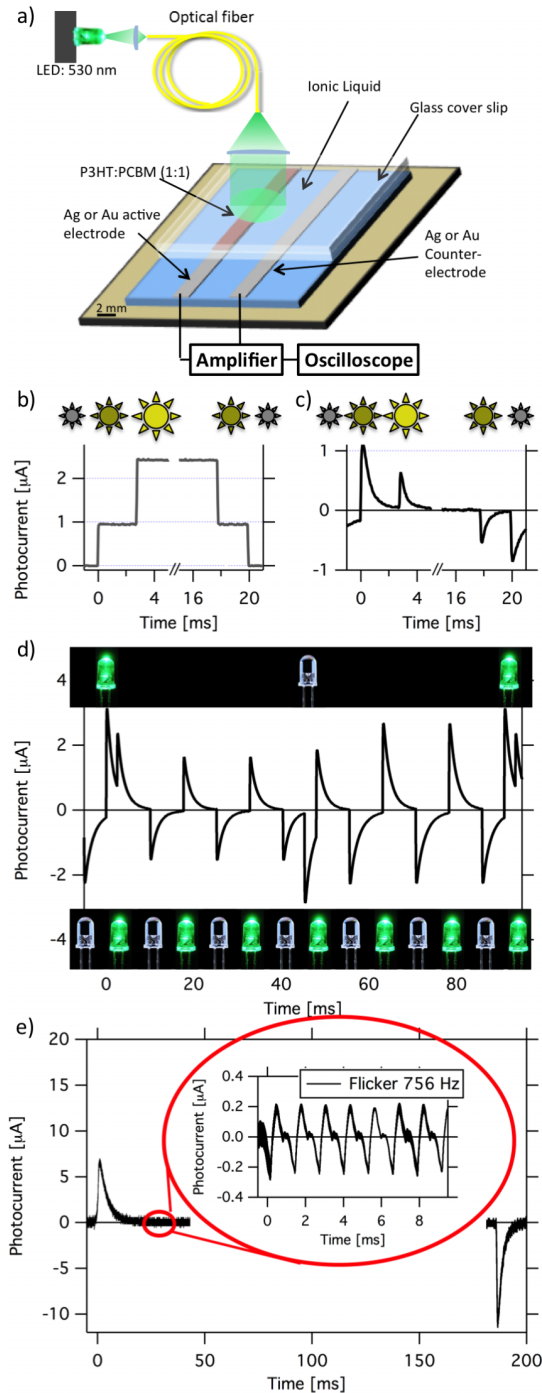


FIG. 1. (a) Scale drawing of the IL-MISM devices used in this study; (b) detection of changes in light intensity in a SiPD, and (c) a MISM photodetector (see ESI¹⁸ p2), by increasing the illumination from 0 μW to 120 μW , and further to 310 μW ; (d) simultaneous resolution of two modulated light sources (LED 530 nm, 200 μW , square-wave modulated at 50% duty, primary 11 Hz, secondary, 66 Hz, offset = 2.5); (e) resolution of the imperceptible flickering in a commercial filament bulb by an MISM device.

to indicate the health and lifetime of light source, it clearly demonstrates the intrinsic improvement in the resolution of modulated signals, compared to MSM devices, which is highly applicable to optical communication, where optical signals are rarely modulated at a depth of 100%, but as fractional perturbations to a CW source.

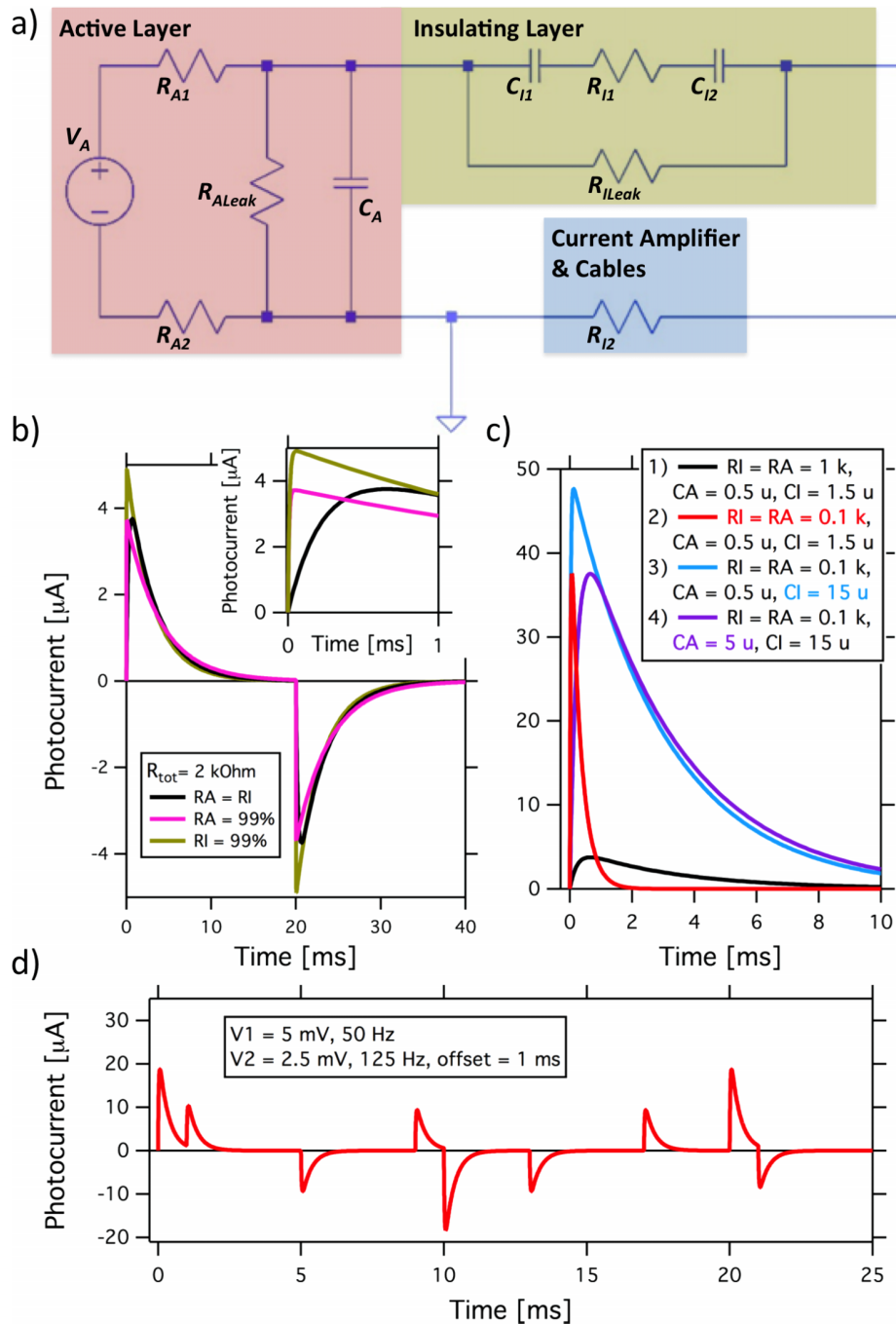


FIG. 2. (a) Proposed equivalent circuit of the MISM photodetector. (b-d) Simulated response over a 10Ω resistor to a square-wave voltage signal (10 mV), leakage resistances of $10 \text{ M}\Omega$, $C_A = 0.5 \text{ }\mu\text{F}$, $C_I = 1.5 \text{ }\mu\text{F}$, $R_I = R_A = 100 \Omega$, unless otherwise stated in the legend. For simplicity the resistance of the measurement device (amplifier and cables) are added to R_I . Color coding persists through all subfigures. (b) Effect of splitting the resistance in the device equally, or mainly onto the active layer or insulating layer; (c) effect of decreasing the total series resistance (1-2), increasing the insulating layer capacitance (2-3), and increasing the active layer capacitance (3-4); (d) simulation of multiple signal detection (c.f. Fig. 1(d)) using two voltage sources in series, in place of V_A in Fig. 2(a).

The operation of a photodetector reacting to changes in light intensity, as opposed to light intensity itself, can be understood when looking at the proposed equivalent circuit (Figure 2(a)). The active layer essentially characterizes a low-pass filter, containing a voltage source V_A in series with a resistor R_A (the use of two resistors instead of one helps with subsequent discussion) and

in parallel with a capacitor C_A . The in-series connection of the capacitor C_I and resistor R_I of the insulating layer (again the specific illustration via two capacitors is only to aid discussion), changes the device essentially to that of a band-pass filter.

Using computer simulation,¹³ as well as building this circuit from commercially available components, the distinct rise and decay of the photocurrent transient can be simulated, and the influence of the individual components studied (Figure 2(b)-2(d) and Supporting Information¹⁸ Figures S4-S6). While the leakage of the active layer R_{ALeak} has little effect on signal shape, but greatly reduces the overall signal intensity, the leakage of the insulating layer R_{ILeak} allows the passage of a DC current during the period of applied voltage, which eventually changes to a square wave signal (Supporting Information¹⁸ Figure S4). This leakage current can become significant when using liquid insulating layers (ionic liquids, electrolyte solutions). *Ad extremum*, by adding a charge transport pathway through the insulator layer via an appropriate redox couple, the leakage can be total, essentially turning the detector into a dye-sensitized solar cell.^{14,15}

The total series resistance in the device $R_A + R_I$ strongly affects the signal magnitude, as $I = V/R$, as well as the decay time of the response [$(R_A + R_I) \times C_I$] (Figure 2(c) (1-2)). In contrast, the rise-time of the signal is essentially only affected by the smaller resistor, and is thus strongly influenced by the relative balance of R_A to R_I ($R \times C_A$, with R being the smaller of the two resistors) (Figure 2(b)).

The amount of charge $Q = Q_A + Q_I$ stored internally in the device is directly proportional to the sum capacitance of the layers $Q = V_A \times (C_A + C_I)$. Thus, if the total capacitance is increased the total charge is increased. This, however, only results in increased photocurrent if that additional charge is stored at the insulating layer capacitor, as the storage of charge within the active layer is non-contributing (Figure 2(c) (3-4)).

The proposed equivalent circuit can easily explain the operation under high background light conditions, and the detection of light signals from multiple sources (Figure 2(d)). The primary light source generates a certain photovoltage in the active layer V_{AI} , which charges, on the one hand, the capacitor of the active layer, and on the other, the capacitor of the insulating layer. If a secondary light source then illuminates the detector, the generated photovoltage is increased $V_{AI} + V_{A2}$, leading to the charging of the already pre-charged capacitors. In simulation, the shape of the transient waveform is identical for the primary and secondary light pulse, and the signal amplitude is directly proportional to the voltage applied (Supporting Information¹⁸ Figure S6). This is not the case for the MISM device (Figures 1(c) and 3) due, in part, to the effect of light and electric field on the electronic properties of the active layer, and it is important to discuss the implications of these effects in more detail.

The best measure for the generated photovoltage is the total charge accumulated at the insulating layer capacitor, as essentially $Q_I = V_A/C_I$. As can be seen in Figure 3(a)-3(b), a sublinear dependence of the charge on light power P can be observed. The degree of sublinearity depends on the specifics of the device, but a sublinear behavior has been observed for all MISM devices studied to date. While all devices could be fitted with a power dependency ($Q_I \sim a \cdot (P^\gamma - 1)$, where $\gamma < 1$, for Fig. 3(b) $\gamma = 0.8$), the origin of the sublinearity can only be speculated upon, and would require more in-depth study over a wider range of light intensities, with the extraction of other parameters. However, it is likely related to the logarithmic dependence of open-circuit voltage V_{OC} on light intensity, previously characterized for MSM bulk heterojunction devices.¹⁶ Moreover, as the number of free carriers increases with increasing light intensity, the resistance of the active layer decreases. Therefore, it is not surprising that the dependence on signal intensity can appear more linear, as $I_{max} \approx V_A/R$ (Figure 3(b)). The decrease in resistance in the active layer is also evident from the faster decay times of the devices under stronger illumination (Figure 3(c)).

The decreased resistance in the active layer has a similar effect on the transient induced by the secondary light source. Also here, not only the total charge (and thus the increase in photovoltage) is reduced with the degree of pre-illumination, but also the resistance of the active layer, as evident by the faster rise and decay times of the response (Figure 3(d)-3(f)).

Furthermore, the contact of the two layers is essential, when considering the effect the strong electric field at the S/I interface could have on the charge separation efficiency (and therefore the generation of a photovoltage), as well as charge mobility within the active layer. When considering

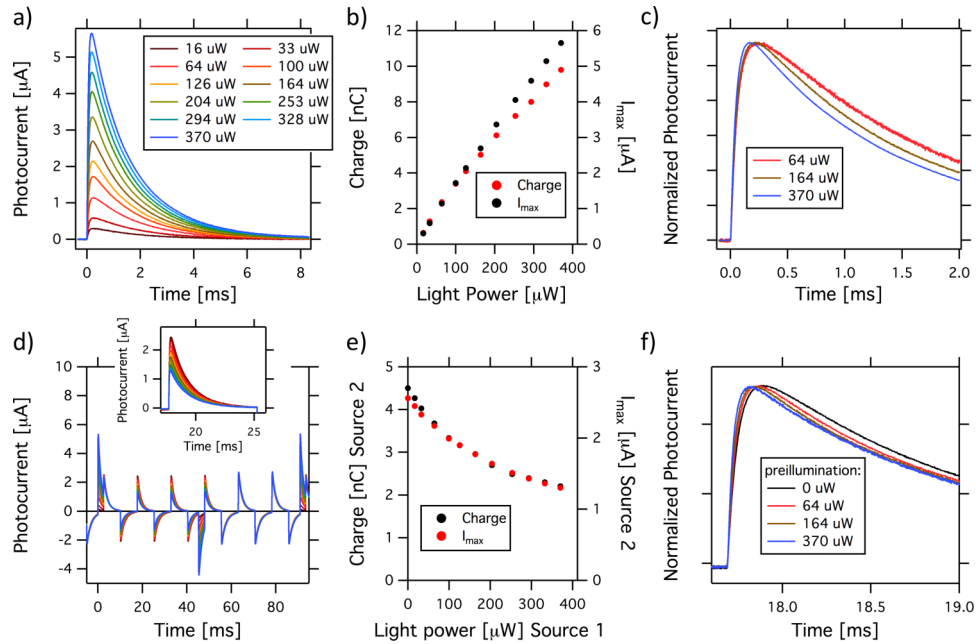


FIG. 3. (a) Effect of (primary) light source intensity on the waveform of an MISM photodetector (see ESI¹⁸ p2). Color coding persists through all subfigures. (b) Extracted total charge Q and peak intensity I_{max} from (a), displaying a sublinear dependence on light intensity; (c) normalized photocurrent signal of selected waves of (a), showing the decrease in rise and fall times with increasing light intensity; (d) effect of the light intensity of the primary signal (see (a)) on the waveform resulting from the secondary light source of 190 μW (inset displays an expansion of the secondary light response) showing a decrease in intensity with increasing pre-illumination; (e) extracted Q and I_{max} from (d); (f) normalized response from selected waves of (d), showing the decrease in rise and fall time with increasing pre-illumination. Primary and secondary light source modulations are identical to those described in Fig.1(d).

the equivalent circuit, it is clear that the MISM functionality could be replicated with a composite of an MSM device and high-pass filter, with no decrease in performance, if the internal S/I interface had no positive effect on the device performance. However, when a thin layer of metal (5 nm Au) is introduced between the active layer and insulating layer, the photoresponse in the MISM-photodetector is greatly reduced, compared to a device without the metal (Figure 4 and Supporting Information¹⁸ Figure S7). Over time, the ionic liquid can penetrate the thin metal layer, whereupon the photoresponse recovers to a level comparable to a device without the metal interlayer (Figure 4). This suggests that the strong electric field at the interface with the active layer can increase the charge separation and extraction efficiency within such devices, and therefore enhance their performance.

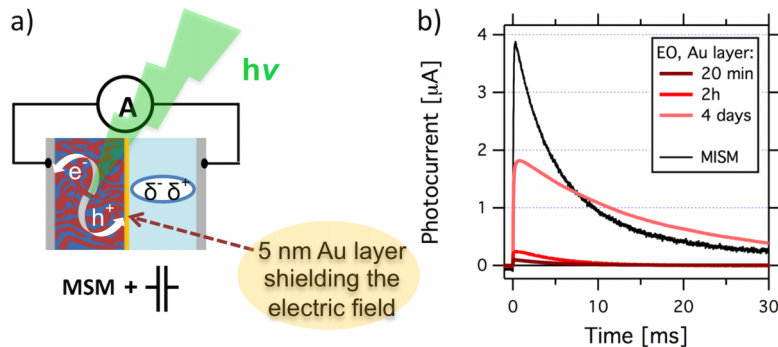


FIG. 4. (a) Pictorial representation of an MISM where the electrostatic field at the S/I interface is shielded by the insertion of a 5 nm Au interlayer between the active layer and insulator layer; (b) its effect on the photoresponse over time in operation, using the ionic liquid EMIM-Otf (EO) as insulator, which is known to induce swelling of the P3HT:PCBM layer.

In conclusion, the insertion of an insulating layer into a standard MSM photodetector changes the nature of the device photoresponse, reacting only to changes in light intensity, as opposed to light intensity itself. This new concept might open new possibilities for signal transfer systems, e.g., from imperceptible modulation of ambient lighting in our offices (*cf.* Figure 1). For such systems, high speed (bandwidth) and efficiency (detectivity) are necessary. From this study, it becomes clear that this could be achieved by decreasing the resistances (especially of the active layer), and by exploiting pre-polarized dielectrics, through work-function tuning of the counter electrode, the use of background illumination, or by substitution of the insulator layer with ferroelectric materials.¹⁷

ACKNOWLEDGEMENTS

We thank our former Bachelor student Mori Kotaro for his assistance in device fabrication. We are grateful to the Ministry of Education, Culture, Sports and Technology (MEXT) of Japan for a Grant-in-Aid for Scientific Research. L.R. thanks the Japan Society for the Promotion of Science (JSPS) for a postdoctoral research fellowship. This work was also supported by the JSPS Core-to-Core Program, A. Advanced Research Networks.

- ¹ Y.-L. Loo and I. McCulloch, *MRS Bulletin* **33**(7), 653–705 (2008).
- ² T. Xu and L. Yu, *Materials Today* **17**, 11–15 (2014).
- ³ G. Li, T. Fleetham, E. Turner, X.-C. Hang, and J. Li, *Adv. Optical Mater* **3**, 390–397 (2015).
- ⁴ A. J. Heeger, *Adv. Mater.* **26**, 10–28 (2014).
- ⁵ P. Docampo, S. Guldin, T. Leijtens, N. K. Noel, U. Steiner, and H. J. Snaith, *Adv. Mater.* **26**, 4013–4030 (2014).
- ⁶ K.-J. Baeg, M. Binda, D. Natali, M. Caironi, and Y.-Y. Noh, *Adv. Mater.* **25**, 4267–4295 (2013).
- ⁷ P. Peumans, A. Yakimov, and S. R. Forrest, *J. Appl. Phys.* **93**, 3693–3723 (2003).
- ⁸ L. Hu, Y. Noda, H. Ito, H. Kishida, A. Nakamura, and K. Awaga, *Appl. Phys. Lett.* **96**, 243303 (2010).
- ⁹ S. Dalglish, M. M. Matsushita, L. Hu, B. Li, H. Yoshikawa, and K. Awaga, *J. Am. Chem. Soc* **134**, 12742–12750 (2012).
- ¹⁰ B. Li, S. Dalglish, Y. Miyoshi, H. Yoshikawa, M. M. Matsushita, and K. Awaga, *Appl. Phys. Lett* **101**, 173302 (2012).
- ¹¹ S. Dalglish, L. Reissig, L. Hu, M. M. Matsushita, Y. Sudo, and K. Awaga, *Langmuir* **31**, 5235–5243 (2015).
- ¹² I. B. Vasile, A. Vasile, S. Luciana, and M. Tache, Proc. SPIE, Advanced Topics in Optoelectronics, Microelectronics, and Nanotechnologies III **6635**, 663518 (2007).
- ¹³ LTspice IV (Linear Technologies, www.linear.com).
- ¹⁴ B. O'Regan and M. Grätzel, *Nature* **353**, 737–740 (1991).
- ¹⁵ J. Wu, Z. Lan, J. Lin, M. Huang, Y. Huang, L. Fan, and G. Luo, *Chem. Rev.* **115**, 2136–2173 (2015).
- ¹⁶ L. J. A. Koster, V. D. Mihailetschi, R. Ramaker, and P. W. M. Blom, *Appl. Phys. Lett.* **86**, 123509 (2005).
- ¹⁷ L. Hu, S. Dalglish, M. M. Matsushita, H. Yoshikawa, and K. Awaga, *Nature Comm* **5**, 3279 (2014).
- ¹⁸ See supplementary material at <http://dx.doi.org/10.1063/1.4939921> for Materials and Methods, Supplemental Figures S1-S7, and Further Points of consideration related to the study.